The Daily COVID-19 Literature Surveillance Summary

January 28, 2021

DISCLAIMER

This free and open source document represents a good faith effort to provide real time, distilled information for guiding best practices during the COVID-19 pandemic. This document is not intended to and cannot replace the original source documents and clinical decision making. These sources are explicitly cited for purposes of reference but do not imply endorsement, approval or validation.

This is not an official product or endorsement from the institutions affiliated with the authors, nor do the ideas and opinions described within this document represent the authors' or their affiliated institutions' values, opinions, ideas or beliefs. This is a good faith effort to share and disseminate accurate summaries of the current literature.

NOW LIVE!

Daily audio summaries of the literature in 10 minutes or less.
https://www.covid19lst.org/podcast/

COVID-19 Daily Literature Surveillance

COVID19LST

Bringing you real time, distilled information for guiding best practices during the COVID-19 pandemic

LEVEL OF EVIDENCE

Oxford Centre for Evidence-Based Medicine 2011 Levels of Evidence

Question	Step 1 (Level 1*)	Step 2 (Level 2*)	Step 3 (Level 3*)	Step 4 (Level 4*)	Step 5 (Level 5)
How common is the problem?	Local and current random sample surveys (or censuses)	Systematic review of surveys that allow matching to local circumstances**	Local non-random sample**	Case-series**	n/a
Is this diagnostic or monitoring test accurate? (Diagnosis)	Systematic review of cross sectional studies with consistently applied reference standard and blinding	Individual cross sectional studies with consistently applied reference standard and blinding	Non-consecutive studies, or studies without consistently applied reference standards**	Case-control studies, or "poor or non-independent reference standard**	Mechanism-based reasoning
What will happen if we do not add a therapy? (Prognosis)	Systematic review of inception cohort studies	Inception cohort studies	Cohort study or control arm of randomized trial*	Case-series or case-control studies, or poor quality prognostic cohort study**	n/a
Does this intervention help? (Treatment Benefits)	Systematic review of randomized trials or *n*-of-1 trials	Randomized trial or observational study with dramatic effect	Non-randomized controlled cohort/follow-up study**	Case-series, case-control studies, or historically controlled studies**	Mechanism-based reasoning
What are the COMMON harms? (Treatment Harms)	Systematic review of randomized trials, systematic review of nested case-control studies, *n*-of-1 trial with the patient you are raising the question about, or observational study with dramatic effect	Individual randomized trial or (exceptionally) observational study with dramatic effect	Non-randomized controlled cohort/follow-up study (post-marketing surveillance) provided there are sufficient numbers to rule out a common harm. (For long-term harms the duration of follow-up must be sufficient.)**	Case-series, case-control, or historically controlled studies**	Mechanism-based reasoning
What are the RARE harms? (Treatment Harms)	Systematic review of randomized trials or *n*-of-1 trial	Randomized trial or (exceptionally) observational study with dramatic effect			
Is this (early detection) test worthwhile? (Screening)	Systematic review of randomized trials	Randomized trial	Non -randomized controlled cohort/follow-up study**	Case-series, case-control, or historically controlled studies**	Mechanism-based reasoning

*** Level may be graded down on the basis of study quality, imprecision, indirectness (study PICO does not match questions PICO), because of inconsistency between studies, or because the absolute effect size is very small; Level may be graded up if there is a large or very large effect size.**

**** As always, a systematic review is generally better than an individual study.**

How to cite the Levels of Evidence Table

OCEBM Levels of Evidence Working Group*. "The Oxford 2011 Levels of Evidence".

Oxford Centre for Evidence-Based Medicine. http://www.cebm.net/index.aspx?o=5653

** OCEBM Table of Evidence Working Group = Jeremy Howick, Iain Chalmers (James Lind Library), Paul Glasziou, Trish Greenhalgh, Carl Heneghan, Alessandro Liberati, Ivan Moschetti, Bob Phillips, Hazel Thornton, Olive Goddard and Mary Hodgkinson*

EXECUTIVE SUMMARY

Understanding the Pathology

- Virology experts from several Chinese institutions analyzed sera from 104 patients with severe COVID-19 admitted to Wuhan Jinyitan Hospital between January 17 and March 30, 2020. They found evidence that neutralizing antibodies (nAb) to SARS-CoV-2 persisted beyond 6 months while immunoglobulin (IgG) against receptor binding domains (RBD) and nucleocapsid protein (N) decreased from the acute infection phase to the convalescent phase. Authors suggest further studies with increased sample size and longer follow-up may help determine nAb's role in long-term immunity and contribute to vaccine development.

TABLE OF CONTENTS

ADULTS

VENOUS THROMBOEMBOLISM AND MAJOR BLEEDING IN PATIENTS WITH COVID-19: A NATIONWIDE POPULATION-BASED COHORT STUDY

Dalager-Pedersen M, Lund LC, Mariager T, Winther R, Hellfritzsch M, Larsen TB, Thomsen RW, Johansen NB, Søgaard OS, Nielsen SL, Omland L, Lundbo LF, Israelsen SB, Harboe ZB, Pottegård A, Nielsen H, Bodilsen J.. Clin Infect Dis. 2021 Jan 5:ciab003. doi: 10.1093/cid/ciab003. Online ahead of print.
Level of Evidence: 1 - Local and current random sample surveys (or censuses)

BLUF

Infectious disease specialists from Aalborg University in Denmark used the civil registration system to compare the risk of bleeding complications and venous thromboembolisms (VTE) in 9,460 patients with COVID-19 from January 27 - June 1, 2020 to 226,510 non-COVID-19 patients with acute illness in the same time period, and to 16,281 influenza positive patients from 2010-2018. They found 0.4% of SARS-CoV-2 patients (Table 5), 0.3% of non-SARS-CoV-2 patients (Table 2), and 1.0% of influenza patients (Table 3) developed a VTE within 30 days. Risk of major bleeding for SARS-CoV-2 patients was 2.3% for hospitalized patients and 0.5% overall. The study suggests that major bleeding and VTE risk is not substantially increased among patients with SARS-CoV-2 compared with other groups.

ABSTRACT

BACKGROUND: Venous thromboembolism (VTE) is a potentially fatal complication of SARS-CoV-2 infection and thromboprophylaxis should be balanced against risk of bleeding. This study aimed to examine risks of VTE and major bleeding in hospitalized and community-managed SARS-CoV-2 patients compared with control populations. METHODS: Using nationwide population-based registries, 30-day risks of VTE and major bleeding in SARS-CoV-2 positive patients were compared with those of SARS-CoV-2 test-negative patients and with an external cohort of influenza patients. Medical records of all COVID-19 patients at six departments of infectious diseases in Denmark were reviewed in detail. RESULTS: The overall 30-day risk of VTE was 0.4% (40/9,460) among SARS-CoV-2 patients (16% hospitalized), 0.3% (649/226,510) among SARS-CoV-2 negative subjects (12% hospitalized), and 1.0% (158/16,281) among influenza patients (59% hospitalized). VTE risks were higher and comparable in hospitalized SARS-CoV-2 positive (1.5%), SARS-CoV-2 negative (1.8%), and influenza patients (1.5%). Diagnosis of major bleeding was registered in 0.5% (47/9,460) of all SARS-CoV-2 positive individuals and in 2.3% of those hospitalized. Medical record review of 582 hospitalized SARS-CoV-2 patients observed VTE in 4% (19/450) and major bleeding in 0.4% (2/450) of ward patients, of whom 31% received thromboprophylaxis. Among intensive care patients (100% received thromboprophylaxis), risks were 7% (9/132) for VTE and 11% (15/132) for major bleeding. CONCLUSIONS: Among people with SARS-CoV-2 infection in a population-based setting, VTE risks were low to moderate and were not substantially increased compared with SARS-CoV-2 test-negative and influenza patients. Risk of severe bleeding was low for ward patients, but mirrored VTE risk in the intensive care setting.

Table 5: Risk of venous thromboembolism, major bleeding, and death by medical record review of patients hospitalized with SARS-CoV-2 at six departments of infectious diseases in Denmark, 2020.

		Non-ICU		ICU
	Total	Anticoagulant therapy	No anticoagulant therapy	Anticoagulant therapy[a]
Observations	**N=582**	**N=140**	**N=310**	**N=132**
VTE during admission or follow-up, n (% of N)	28 (5)	4 (3)	15 (5)	9[b] (7)
Pulmonary embolism	24 (4)	4 (3)	11[c] (4)	9[b] (7)
Deep vein thrombosis	6[d] (1)	0	4 (1)	2 (1)
Major bleeding during admission, n (% of N)	17 (3)	2[e] (1)	0	15[e] (11)
CNS, retroperitoneal or intraocular hemorrhage	3 (1)	0	0	3 (2)
Transfusion >1 unit of blood or significant intervention required	13 (2)	2 (1)	0	11 (8)
Hemorrhage as a contributing factor to death	3 (1)	0	0	3 (2)
In-hospital mortality, n (% of N)	124 (20)	31 (22)	42 (13)	48 (36)
Patients with VTE before death	4 (1)	1	0	3
Patient with major bleeding during admission before death	7 (1)	0	0	7

Abbreviations: VTE, venous thromboembolism; SARS-CoV-2, severe acute respiratory syndrome corona virus 2; CNS, central nervous system; ICU, intensive care unit. [a] Anticoagulant therapy consisted of standard dose LMWH in 90 patients, intermediate/high dose LMWH in 27 patients, DOACs in 14 patients, and vitamin K antagonist in one patient. [b] Three patients not receiving anticoagulant treatment were diagnosed with pulmonary embolism before they were transferred to the intensive care unit and anticoagulant treatment started. [c] Pre-existing risk factors before diagnosis of VTE were present in four patients (*i.e.* airplane travel within 30 days, active cancer treatment within six months combined with recent surgery within 30 days, hip surgery within 30 days, and previous deep vein thrombosis in one each). [d] Two patients were diagnosed with both deep vein thrombosis and pulmonary embolism. [e] For the two non-ICU patients with major bleeding, anticoagulant therapy consisted of standard dose LMWH in both patients. For the 15 ICU patients with major bleeding, anticoagulant therapy consisted of standard dose LMWH in eight patients, intermediate/high-dose LMWH in five patients, and DOACs in two patients.

Table 3: Registry-based data of 30-day risks of VTE (n/N, %) in SARS-CoV-2 test positive and influenza patients.

	Non-hospitalized			Hospitalized[a]		
Outcome	**SARS-CoV-2 positive**	**Influenza positive**	**Risk difference (95% CI)**	**SARS-CoV-2 positive**	**Influenza positive**	**Risk difference (95% CI)**
VTE (diagnoses only)	17/7,920 (0.2)	11/6,682 (0.2)	0.0 (-0.1 to 0.2)	23/1,540 (1.5)[b]	147/9,599 (1.5)	-0.0 (-0.7 to 0.6)
Deep vein thrombosis	5/7,920 (0.1)	NA	-	7/1,540 (0.5)	NA	-
Pulmonary embolism	12/7,920 (0.2)	NA	-	16/1,540 (1.0)	NA	-
VTE (incl. prescriptions)	24/7,920 (0.3)	-	-	36/1,540 (2.3)	-	-
Major bleeding	11/7,920 (0.1)	32/6,682 (0.5)	-0.3 (-0.5 to -0.2)	36/1,540 (2.3)	234/9,599 (2.4)	-0.1 (-0.9 to 0.7)
VTE in subgroups						
VTE risk factors						
No	NA	NA	-	NA	NA	-
Yes	NA	NA	-	NA	NA	-
Sex						
Female	NA	6/3,696 (0.2)	-	NA	64/4,688 (1.4)	-
Male	NA	5/2,986 (0.2)	-	NA	83/4,911 (1.7)	-
Age						
0-64	10/6,758 (0.1)	5/4,723 (0.1)	0.0 (-0.1 to 0.2)	11/523 (2.1)	49/3,441 (1.4)	0.7 (-0.6 to 1.9)
65+	7/1,162 (0.6)	6/1,959 (0.3)	0.3 (-0.2 to 0.8)	12/1,017 (1.2)	98/6,158 (1.6)	-0.4 (-1.1 to 0.3)
Charlson score						
0	NA	NA	-	NA	NA	-
≥1	NA	NA	-	NA	NA	-

Abbreviations: NA, not applicable as Danish regulations do not allow reporting of less than 5 individuals in each cell; SARS-CoV-2, severe acute respiratory syndrome corona virus 2; VTE, venous thromboembolism. [a]Numbers refers to start of follow-up. A large number of patients were hospitalized at end of follow-up, 201 SARS-CoV-2 positive patients and 2,037 influenza patients. [b]Among hospitalized SARS-CoV-2 patients, VTE was diagnosed in 16/991 from February 27 through March 31 and in 7/549 from April 1 through April 31, 2020.

Table 2: Registry-based data of 30-day risks of VTE (n/N, %) in SARS-CoV-2 test positive or negative patients.

	Non-hospitalized			Hospitalized[a]		
	SARS-CoV-2			SARS-CoV-2		
Outcome	**Positive**	**Negative**	**Risk difference (95% CI)**	**Positive**	**Negative**	**Risk difference (95% CI)**
VTE (diagnoses only)	17/7,920 (0.2)	166/200,379 (0.1)	0.1 (0.0 to 0.2)	23/1,540 (1.5)[b]	483/26,131 (1.8)	-0.4 (-1.0 to 0.3)
Deep vein thrombosis	5/7,920 (0.1)	79/200,379 (0.0)	0.0 (0.0 to 0.1)	7/1,540 (0.5)	117/26,131 (0.4)	0.0 (-0.3 to 0.4)
Pulmonary embolism	12/7,920 (0.2)	87/200,379 (0.0)	0.1 (0.0 to 0.2)	16/1,540 (1.0)	366/26,131 (1.4)	-0.4 (-0.9 to 0.2)
VTE (incl. prescriptions)	24/7,920 (0.3)	206/200,379 (0.1)	0.2 (0.1 to 0.3)	36/1,540 (2.3)	576/26,131 (2.2)	0.1 (-0.6 to 0.9)
Major bleeding	11/7,920 (0.1)	474/200,379 (0.2)	-0.1 (-0.2 to 0.0)	36/1,540 (2.3)	1,170/26,131 (4.5)	-2.1 (-2.9 to -1.3)
VTE in subgroups						
VTE risk factors						
No	NA	90/159,058 (0.1)	-	NA	186/13,341 (1.4)	-
Yes	NA	76/41,321 (0.2)	-	NA	297/12,790 (2.3)	-
Sex						
Female	NA	86/130,171 (0.1)	-	NA	221/13,100 (1.7)	-
Male	NA	80/70,208 (0.1)	-	NA	262/13,031 (2.0)	-
Age						
0-64	10/6,758 (0.1)	91/172,156 (0.1)	0.1 (0.0 to 0.2)	11/523 (2.1)	153/11,608 (1.3)	0.8 (-0.5 to 2.0)
65+	7/1,162 (0.6)	75/28,223 (0.3)	0.3 (-0.1 to 0.8)	12/1,017 (1.2)	330/14,523 (2.3)	-1.1 (-1.8 to -0.4)
Charlson score						
0	NA	133/179,086 (0.1)	-	NA	309/16,096 (1.9)	-
≥1	NA	33/21,293 (0.2)	-	NA	174/10,035 (1.7)	-

Abbreviations: NA, not applicable as Danish regulations do not allow reporting of less than 5 individuals in each cell; SARS-CoV-2, severe acute respiratory syndrome corona virus 2; VTE, venous thromboembolism. [a]Numbers refers to start of follow-up. A large number of patients were hospitalized at end of follow-up, 201 SARS-CoV-2 positive patients and 2,712 SARS-CoV-2 negative patients. [b]Among hospitalized SARS-CoV-2 patients, VTE was diagnosed in 16/991 (1.6%) from February 27 through March 31 and in 7/549 (1.3%) from April 1 through April 30, 2020.

EFFECTIVE VIRUS-NEUTRALIZING ACTIVITIES IN ANTISERA FROM THE FIRST WAVE OF SEVERE COVID-19 SURVIVORS

Han Y, Liu P, Qiu Y, Zhou J, Liu Y, Hu X, Yang Q, Huang R, Wen X, Song H, Yu P, Yang M, Zhang J, Liu WJ, Peng K, Wu G, Zhang D, Zhou X, Wu Y.. JCI Insight. 2021 Jan 21:146267. doi: 10.1172/jci.insight.146267. Online ahead of print.
Level of Evidence: 3 - Local non-random sample

BLUF

Virology experts from several Chinese institutions analyzed sera from 104 patients with severe COVID-19 admitted to Wuhan Jinyitan Hospital between January 17 and March 30, 2020. They found evidence that neutralizing antibodies (nAb) to SARS-CoV-2 persisted beyond 6 months while immunoglobulin (IgG) against receptor binding domains (RBD) and nucleocapsid protein (N) decreased from the acute infection phase to the convalescent phase (Figures 1, 2, 5). Authors suggest further studies with increased sample size and longer follow-up may help determine nAb's role in long-term immunity and contribute to vaccine development.

ABSTRACT

The pandemic of Coronavirus Disease 19 (COVID-19), caused by severe acute respiratory syndrome coronavirus 2 (SARS-CoV-2), has become one of the worst public health crises. However, knowledge about the dynamics of antibody responses in COVID-19 patients is still poorly understood. In this study, we performed serological study with serum specimens collected at the acute and the convalescent phases from 104 severe COVID-19 patients who were the first wave of COVID-19 cases in Wuhan, China. Our findings uncovered that neutralizing antibodies to SARS-CoV-2 are persistent at least for more than 6 months in severe COVID-19 patients, despite that immunoglobulin G (IgG) levels against receptor binding domain (RBD) and nucleocapsid protein (N) IgG declined from the acute to the convalescent phase. Moreover, we demonstrate that the level of RBD-IgG is capable of correlating with SARS-CoV-2-neutralizing activities in COVID-19 serum. In summary, our findings identify the magnitude, functionality and longevity of antibody responses in COVID-19 patients, which sheds light on better understanding of humoral immune response to COVID-19, and would be beneficial for developing vaccines.

FIGURES

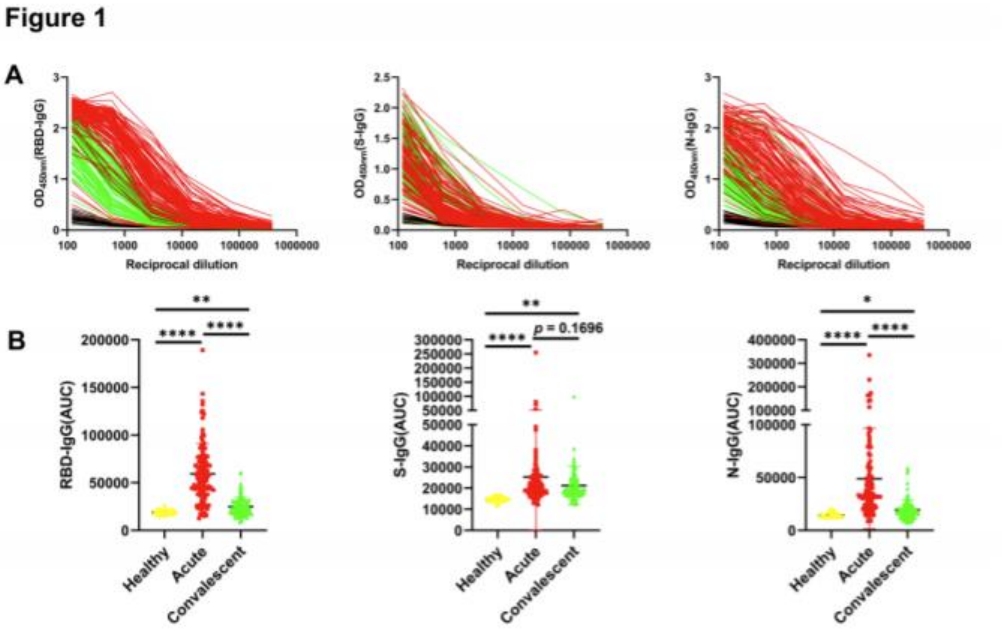

Figure 1. Measure of RBD, S, and N- IgG antibodies in severe COVID-19 patients at the acute and convalescent phases.

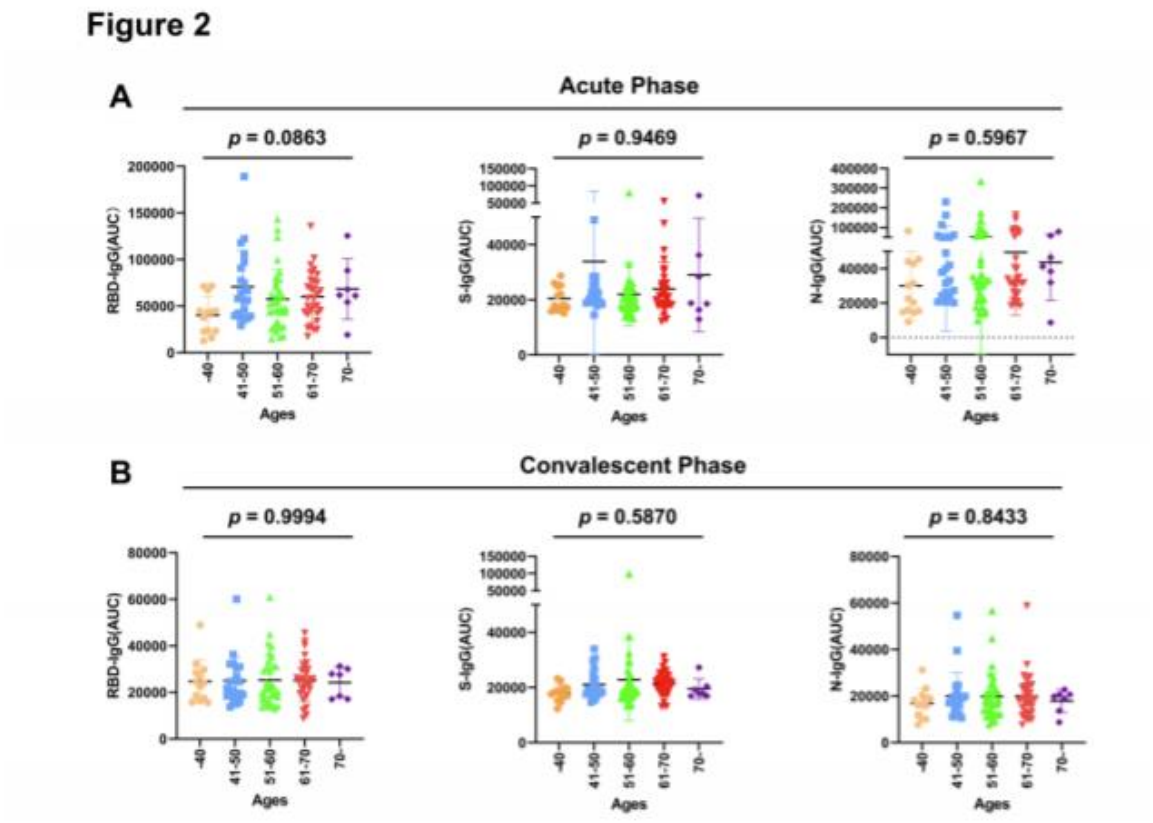

Figure 2. Comparison of RBD, S, and N- IgG antibody levels in different age groups during the acute and convalescent phases

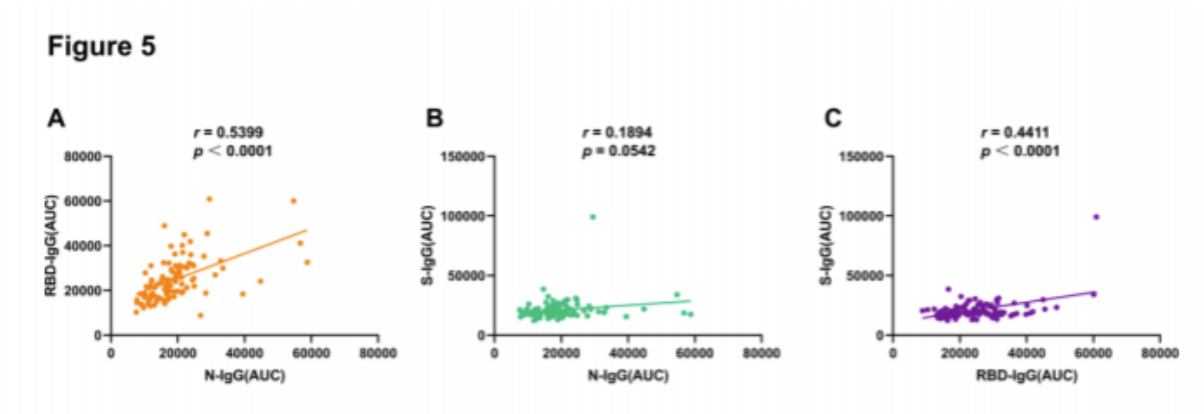

Figure 5. Correlational Analysis of RBD, S, and N- IgG antibodies in severe COVID-19 patients at the convalescent phase

GENOME-WIDE DNA METHYLATION PROFILING OF PERIPHERAL BLOOD REVEALS AN EPIGENETIC SIGNATURE ASSOCIATED WITH SEVERE COVID-19

Corley MJ, Pang APS, Dody K, Mudd PA, Patterson BK, Seethamraju H, Bram Y, Peluso MJ, Torres L, Iyer NS, Premeaux TA, Yeung ST, Chandar V, Borczuk A, Schwartz RE, Henrich TJ, Deeks SG, Sacha JB, Ndhlovu LC.. J Leukoc Biol. 2021 Jan 19. doi: 10.1002/JLB.5HI0720-466R. Online ahead of print.
Level of Evidence: 3 - Local non-random sample

BLUF

A multidisciplinary team of immunology and genomics experts from several American universities compared DNA methylation (DNAm) in patients with severe COVID-19 (n=9), influenza A or B (n=5), HIV-1 (n=9), mild/moderate COVID-19 with HIV coinfection (n=9), and healthy controls (n=9). They found patients with severe COVID-19 had hypermethylation of regulatory regions for IFN response genes (Fig. 1E), significantly increased DNAm inferred neutrophil to lymphocyte ratio (Fig. 1B), and greatly increased epigenetic age of immune cells and tissues (Fig. 2A) compared to other patients. Authors suggest SARS-CoV-2 alters the host epigenome via DNAm and significantly ages immune cells, leaving a reshaped peripheral blood and tissue immune landscape with a genetically altered inflammatory state that could be targeted therapeutically.

ABSTRACT

The global pandemic caused by the severe acute respiratory syndrome coronavirus 2 (SARS-CoV-2) is a highly pathogenic RNA virus causing coronavirus disease 2019 (COVID-19) in humans. Although most patients with COVID-19 have mild illness and may be asymptomatic, some will develop severe pneumonia, acute respiratory distress syndrome, multi-organ failure, and death. RNA viruses such as SARS-CoV-2 are capable of hijacking the epigenetic landscape of host immune cells to evade antiviral defense. Yet, there remain considerable gaps in our understanding of immune cell epigenetic changes associated with severe SARS-CoV-2 infection pathology. Here, we examined genome-wide DNA methylation (DNAm) profiles of peripheral blood mononuclear cells from 9 terminally-ill, critical COVID-19 patients with confirmed SARS-CoV-2 plasma viremia compared with uninfected, hospitalized influenza, untreated primary HIV infection, and mild/moderate COVID-19 HIV coinfected individuals. Cell-type deconvolution analyses confirmed lymphopenia in severe COVID-19 and revealed a high percentage of estimated neutrophils suggesting perturbations to DNAm associated with granulopoiesis. We observed a distinct DNAm signature of severe COVID-19 characterized by hypermethylation of IFN-related genes and hypomethylation of inflammatory genes, reinforcing observations in infection models and single-cell transcriptional studies of severe COVID-19. Epigenetic clock analyses revealed severe COVID-19 was associated with an increased DNAm age and elevated mortality risk according to GrimAge, further validating the epigenetic clock as a predictor of disease and mortality risk. Our epigenetic results reveal a discovery DNAm signature of severe COVID-19 in blood potentially useful for corroborating clinical assessments, informing pathogenic mechanisms, and revealing new therapeutic targets against SARS-CoV-2.

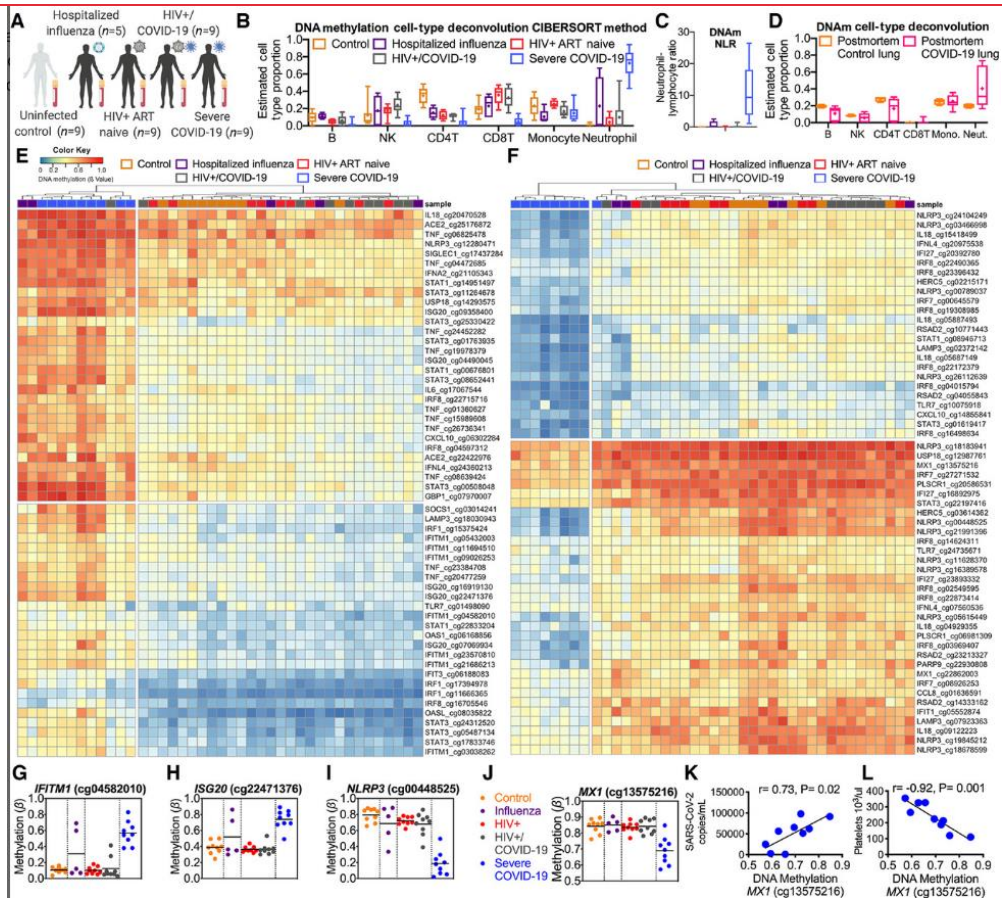

FIGURE 1

DNA methylation signature associated with severe COVID-19. (A) Overview of experimental design for comparative DNA methylation profiling. (B) Box and whisker plots of DNA methylation cell type deconvolution by the CIBERSORT method21 showing estimated cell type proportions of B cells, NK cells, CD4 T cells, CD8 T cells, monocytes, and neutrophils for uninfected control (orange), hospitalized influenza (purple), primary HIV+ ART naïve (red), coinfection HIV+/COVID-19 (gray), and severe COVID-19 (blue) PBMCs. (C) DNA methylation (DNAm)-based neutrophil–lymphocyte ratio (NLR). (D) Box and whisker plots of DNA methylation cell-type deconvolution showing estimated cell-type proportions of B cells, NK cells, CD4 T cells, CD8 T cells, monocytes, and neutrophils in postmortem lung tissues from COVID-19 and uninfected controls. (E) Heatmap of hypermethylated CpGs in uninfected control (orange), hospitalized influenza (purple), primary HIV+ ART naïve (red), coinfection HIV+/COVID-19 (gray), and severe COVID-19 (blue) PBMCs; each participant indicated at top of row. GeneID associated with each CpG displayed for each row. Unsupervised hierarchic clustering above columns identified 2 main clusters. Methylation values displayed as ranging from low methylation (0; blue) to high methylation (1, red). (F) Heatmap of hypomethylated CpGs in uninfected control (orange), hospitalized influenza (purple), primary HIV+ ART naïve (red), coinfection HIV+/COVID-19 (gray), and severe COVID-19 (blue) PBMCs. GeneID associated with each CpG displayed for each row. Unsupervised hierarchic clustering above columns identified 2 main clusters. Methylation values displayed as ranging from low methylation (0; blue) to high methylation (1, red). (G–J) Dot plots of DNA methylation levels at CpGs related to IFITM1, ISG20, NLRP3, and MX1 genes. (K and L) Correlation plots of SARS-CoV-2 plasma viral copies/ml and platelets count with DNA methylation levels of CpG at the MX1 genes

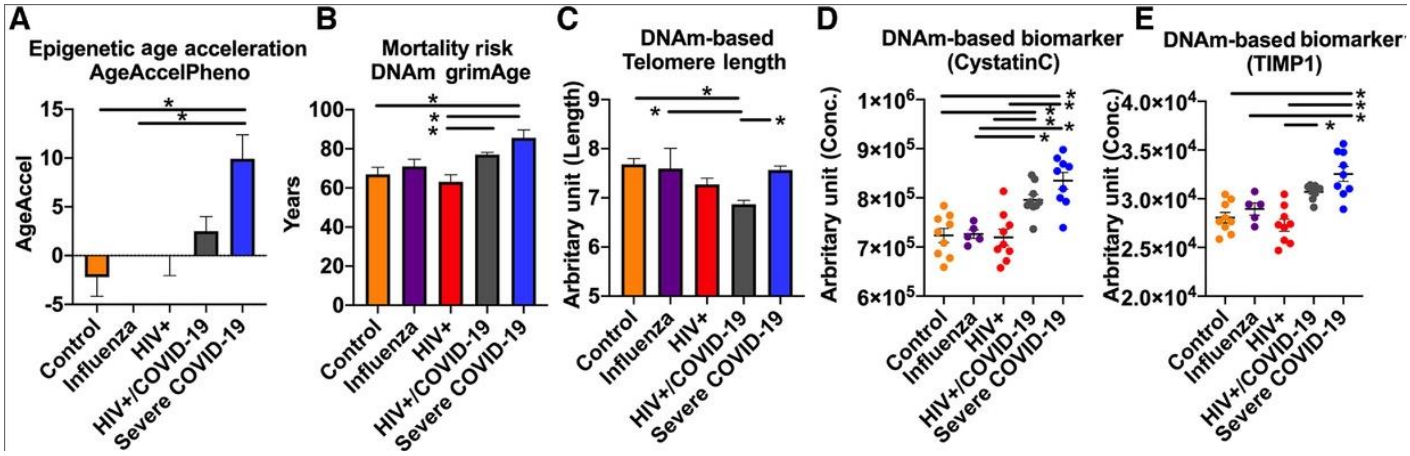

FIGURE 2

Comparative epigenetic clock analyses of uninfected controls, influenza infection, primary HIV infection, HIV+/COVID-19 coinfection, and severe COVID-19. (A) Bar graph displaying significant elevation in estimated epigenetic age acceleration in severe COVID-19 participants compared to uninfected controls and influenza. (B) Bar graph displaying significant elevation in estimated mortality risk according to DNAm GrimAge30 in severe COVID-19 participants compared with uninfected controls and primary HIV. (C) Bar graph displaying significant decrease in DNAm-based telomere length in primary HIV compared with uninfected control. (D and E) Scatter plot showing severe COVID-19 participants significant elevations in DNAm-based biomarker estimates of cystatin C and TIMP1 compared with uninfected control, influenza, HIV+, and coinfection HIV+/COVID-19. One-way ANOVA was utilized to identify significant group differences. Post hoc multiple comparisons testing utilized Tukey test. Significance was set at P = 0.05

COVID-19-ASSOCIATED COAGULOPATHY

Görlinger K, Levy JH.. Anesthesiology. 2021 Jan 8. doi: 10.1097/ALN.0000000000003688. Online ahead of print.
Level of Evidence: 5 - Opinion

BLUF

Anesthesiologists from University Hospital Essen/Tem Innovations GmbH in Germany and Duke University in the United States introduce an article by Heinz, et al about fibrinolysis and platelet aggregation in severely ill COVID-19 patients. They summarize Heinz, et al's findings showing fibrinolysis resistance with hypercoagulability and tPA resistance (see summary), which apparently contradicts other studies regarding slightly decreased platelet aggregation due to ADP stimulation. Though the study has some limitations, the authors imply the Heinz, et al study contributes to a growing body of literature describing hemostasis profiles of COVID-19 patients that will improve management of hypercoagulability associated with COVID-19.

SUMMARY

The authors offered the following summary of the findings by Heinz, et al:

- "Fibrinolysis resistance in tPA-thromboelastometry was associated with increased plasmin-activator inhibitor-1 concentrations"
- "With severe COVID-19…maximum lysis within a 60-min runtime of less than 3.5%"
- "Both thromboelastography (area under the receiver operating characteristics curve [AUC], 0.74 [95% CI, 0.58 to 0.9]; P = 0.021) and thromboelastometry (AUC, 0.8 [95% CI, 0.7 to 0.9]; P = 0.001) confirmed that hypofibrinolysis was associated with an enhanced incidence of thrombosis"
- "Viscoelastic testing is reported to be superior to standard plasmatic coagulation tests such as activated partial thromboplastin time and prothrombin time in predicting thrombosis in COVID-19"

IN VITRO

FURIN CLEAVAGE OF SARS-COV-2 SPIKE PROMOTES BUT IS NOT ESSENTIAL FOR INFECTION AND CELL-CELL FUSION

Papa G, Mallery DL, Albecka A, Welch LG, Cattin-Ortolá J, Luptak J, Paul D, McMahon HT, Goodfellow IG, Carter A, Munro S, James LC.. PLoS Pathog. 2021 Jan 25;17(1):e1009246. doi: 10.1371/journal.ppat.1009246. Online ahead of print.
Level of Evidence: 5 - Mechanism-based reasoning

BLUF

Molecular biologists and virologists from the Medical Research Council Laboratory of Molecular Biology in Cambridge conducted an in vitro analysis of the role of furin and TMPRSS2 in viral -host membrane fusion of SARS-CoV-2. They found furin enhances TMPRSS2 processing, but CRISPR-Cas9 furin knockouts only reduced, but did not prevent, the production of SARS-CoV-2 virus (Figure 4). Authors suggest that furin plays a non-essential role in the entry of SARS-CoV-2 into cells, and furin inhibitors may decrease viral spread but not completely prevent it.

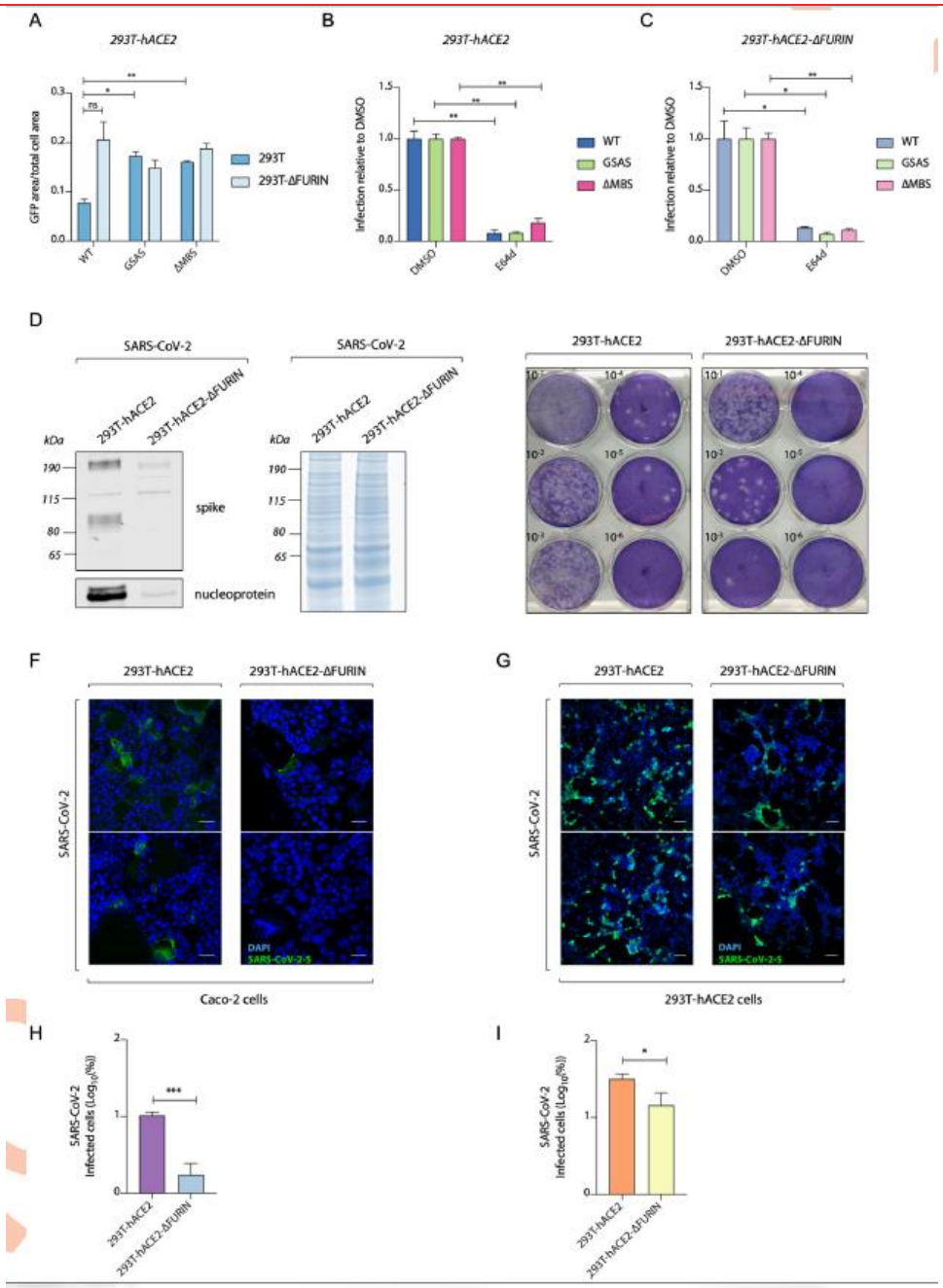

Figure 4. Furin enhances SARS-CoV-2 replication but is not essential for S-pseudovirus entry. (A) Infection of 293T-hACE2 cells with GFP expressing HIV pseudotyped with SARS-CoV-2 S mutants, measured as proportion of cell area expressing GFP. Viruses were produced in either 293T-wt or 293T-ΔFURIN cells. (B) and (C) Infection data of 293T-hACE2 cells with HIV pseudotyped with SARS-CoV-2 S mutants as in (A), with cells pre-treated for 2 hours with either DMSO or 25μMlysosomal inhibitor E64d as indicated. Statistical analysis was performed using Student t-test ﷺP<0.05; ﷺﷺP<0.01, “ns” not significant. (D) Representative western blot of viral particles produced from SARS-CoV-2 infection of 293T-hACE2 and 293T-hACE2-ΔFURIN cells at 72 hours
post infection. Spike and nucleoprotein are detected (left panel). Total protein content of virus preparation by Coomassie staining (right panel). (E) Plaque assay of Vero-hACE2-TMPRSS2 infected with viruses produced in D. (F) and (G) Immunofluorescence images displaying infection of Caco2 BVDV-Npro cells (F) and 293T-hACE2 (G) with equalised amounts of SARS-CoV-2 virus produced in 293T-hACE2 and 293T-hACE2-ΔFURIN cells. Spike (green) and nuclei (blue) are shown. Scale bar, 50 μm. (H) and (I) Quantification of SARS-CoV-2 infected cells shown in (F) and (G). ﷺP<0.05; ﷺﷺﷺ, P<0.001 analysed using Student t-test. Data are expressed as mean +/- SEM (n = 2).

SARS-COV-2 INDUCES ROBUST GERMINAL CENTER CD4 T FOLLICULAR HELPER CELL RESPONSES IN RHESUS MACAQUES

Shaan Lakshmanappa Y, Elizaldi SR, Roh JW, Schmidt BA, Carroll TD, Weaver KD, Smith JC, Verma A, Deere JD, Dutra J, Stone M, Franz S, Sammak RL, Olstad KJ, Rachel Reader J, Ma ZM, Nguyen NK, Watanabe J, Usachenko J, Immareddy R, Yee JL, Weiskopf D, Sette A, Hartigan-O'Connor D, McSorley SJ, Morrison JH, Tran NK, Simmons G, Busch MP, Kozlowski PA, Van Rompay KKA, Miller CJ, Iyer SS.. Nat Commun. 2021 Jan 22;12(1):541. doi: 10.1038/s41467-020-20642-x.
Level of Evidence: 5 - Mechanism-based reasoning

BLUF

Immunologists from the University of California Davis and San Diego investigated immune responses after SARS-CoV-2 infection in rhesus macaques who received either convalescent plasma, normal plasma, or no infusion (Figure 1). In all groups, they found that SARS-CoV-2 infection stimulated a robust Th1-Tfh response (Figure 3), Tfh responses against spike and nucleocapsid protein in lymph nodes (Figure 8), and a primarily IgG response. The authors argue these findings should inform vaccine development, suggesting effective vaccine candidates will induce strong CD4 Th1-Tfh responses.

ABSTRACT

CD4 T follicular helper (Tfh) cells are important for the generation of durable and specific humoral protection against viral infections. The degree to which SARS-CoV-2 infection generates Tfh cells and stimulates the germinal center (GC) response is an important question as we investigate vaccine induced immunity against COVID-19. Here, we report that SARS-CoV-2 infection in rhesus macaques, either infused with convalescent plasma, normal plasma, or receiving no infusion, resulted in transient accumulation of pro-inflammatory monocytes and proliferating Tfh cells with a Th1 profile in peripheral blood. CD4 helper cell responses skewed predominantly toward a Th1 response in blood, lung, and lymph nodes. SARS-CoV-2 Infection induced GC Tfh cells specific for the SARS-CoV-2 spike and nucleocapsid proteins, and a corresponding early appearance of antiviral serum IgG antibodies. Collectively, the data show induction of GC responses in a rhesus model of mild COVID-19.

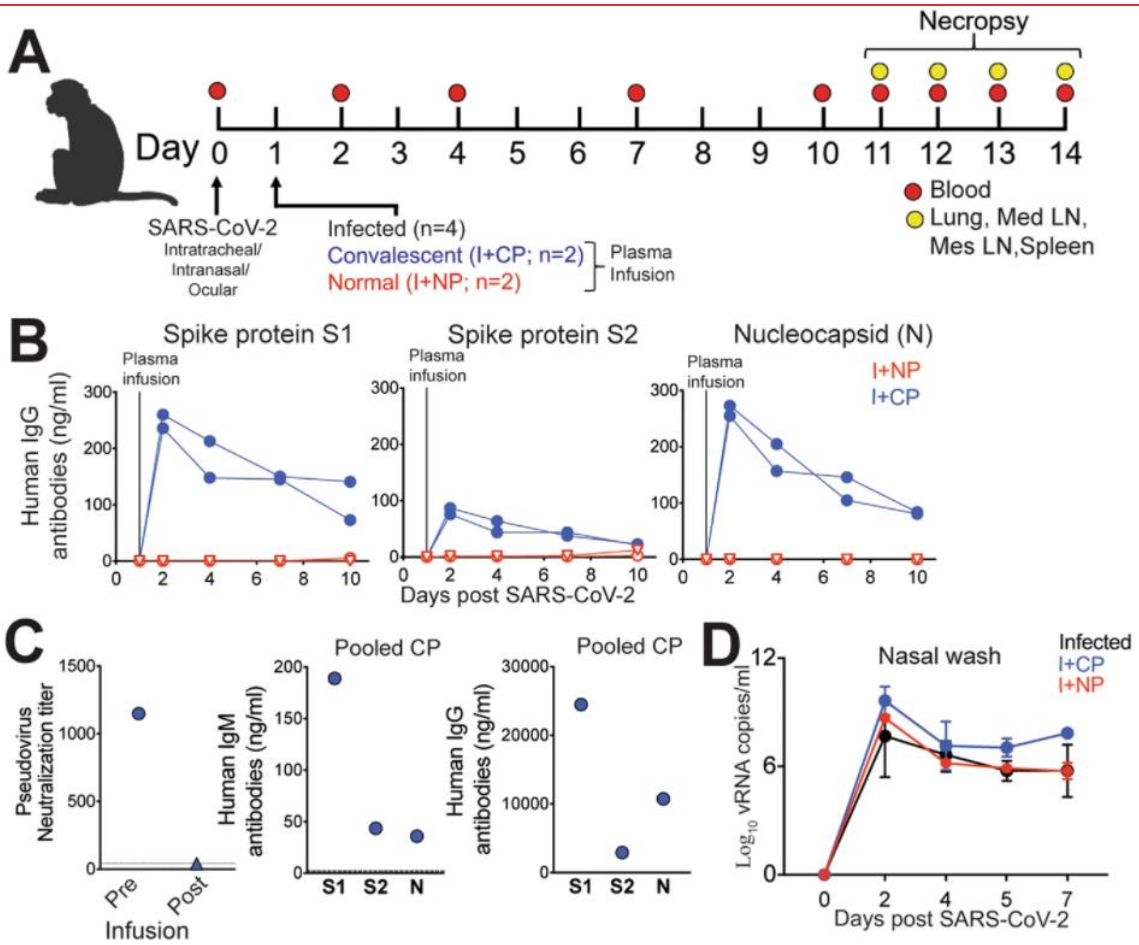

A Rhesus macaques inoculated with severe acute respiratory syndrome coronavirus 2 (SARS-CoV-2) were infused with COVID-19 convalescent plasma (I + CP), normal plasma (I + NP), or did not receive plasma (infected). **B** Concentrations of human IgG antibodies against S1, S2, and N following CP infusion. **C** Concentrations of human IgM and IgG antibodies against S1, S2, and N in pooled CP pre-infusion. Pseudovirus neutralization of CP pre-infusion and pooled macaque sera post infusion. **D** Mean viral RNA (+SD) in nasal washes (kinetic data shown derived from independent animals, sample size for experimental groups: $n = 4$ infected, $n = 2$ I + CP, and $n = 2$ I + NP).

Fig. 1: Experimental design and convalescent plasma infusion.

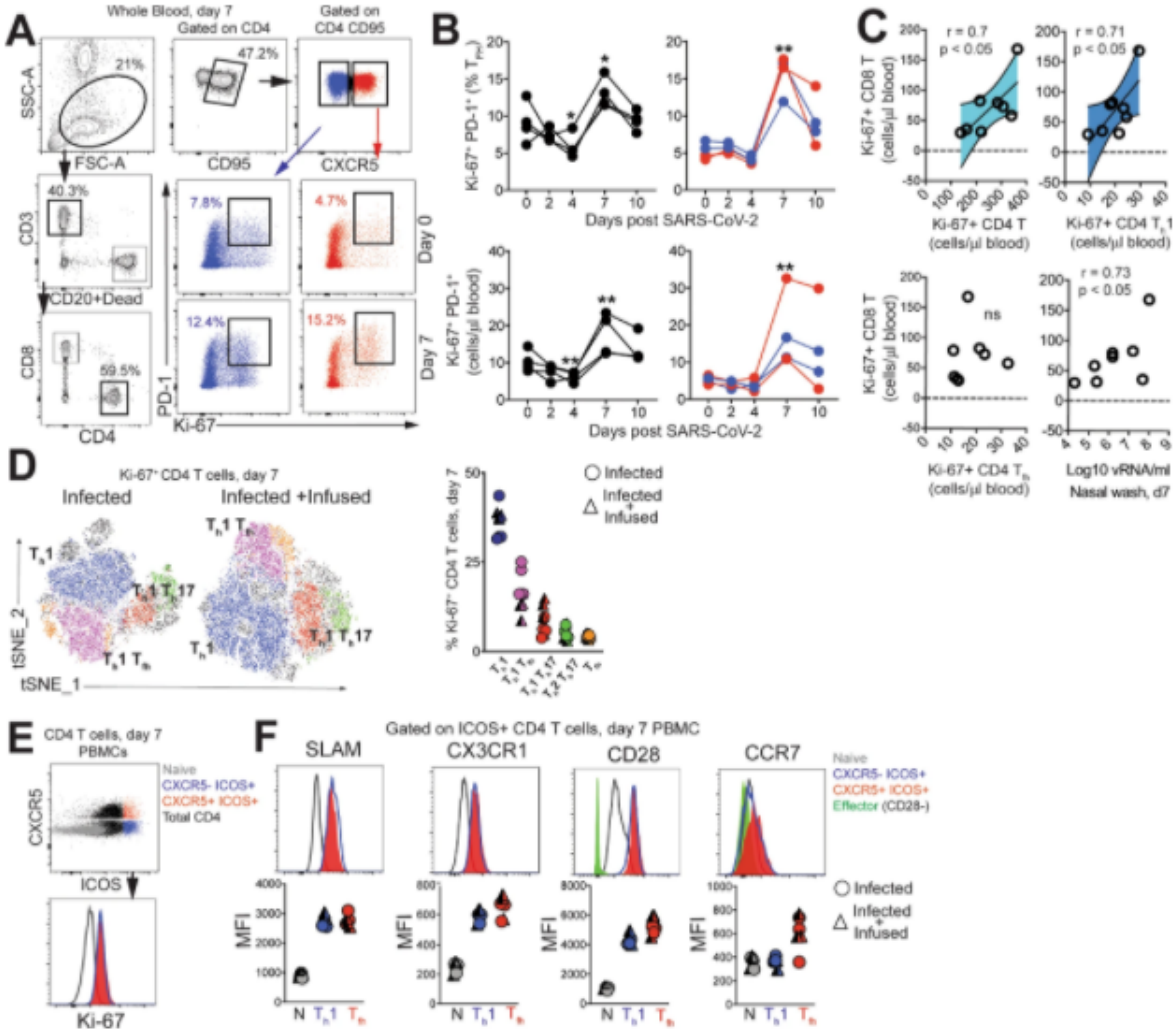

A Representative gating strategy to capture CD4 T cells expressing Ki-67 and programmed death-1 (PD-1) in whole blood. Fluorochromes used were CD3-A700, CD20/Dead-APC-Cy7, CD8-BUV 805, CD4-BV650, CD95-BUV737, CXCR5-PE, PD-1-Pe Cy7, Ki-67-A488, CXCR3-BV786, CCR6-PECF594, CCR4-BV605, SLAM-A488, CX3CR1-PECF594, CD28-Pe-Cy7, CCR7-BV711, ICOS-BV786. **B** Kinetics show frequency and absolute counts of Ki-67$^+$ PD-1$^+$ CD4 T follicular helper cells (T_{fh}) cells (% of T_{fh} cells; $^*p = 0.01$ at d4 and d7 relative to d0 for infected and $^{**}p = 0.002$ at d7 relative to d0 for infused using a one-tailed paired *t* test, absolute T_{fh} cell counts; $^{**}p = 0.003$ at d4 and $^{**}p = 0.0086$ at d7 relative to d0 for infected and $^{**}p = 0.003$ at d7 relative to d0 for infused using a one-tailed paired *t* test. Data are from a real-time longitudinal staining of whole blood performed a single time) **C** correlation plots of Ki-67$^+$CD8 T cells against Ki-67$^+$ CD4 subsets, and viral(v)RNA (all day 7) (two-tailed Pearson test *p* values shown. 95% confidence bands of the best fit line are shown) **D** t-distributed stochastic neighbor embedding (tSNE) plot based on flow cytometry data of CD4 Ki-67$^+$ events at Day 7 from infected (16,197 events) and infected + infused animals (22,406 events); dot plot shows frequency of Ki-67$^+$ CD4 T-cell subsets. (**E**–**F**) Histograms and median fluorescence intensity (MFI) dot plots illustrate relative expression of signaling lymphocyte activation molecule (SLAM), CX3C chemokine receptor 1 (CX3CR1), CD28, and C-C chemokine receptor type 7(CCR7) within four different populations identified at Day 7 in peripheral blood mononuclear cells (PBMCs, $n = 7$). Unique symbols identify animals in each of the experimental groups.

Fig. 3: SARS-CoV-2 infection increases the number CD4 T follicular helper cells in peripheral blood.

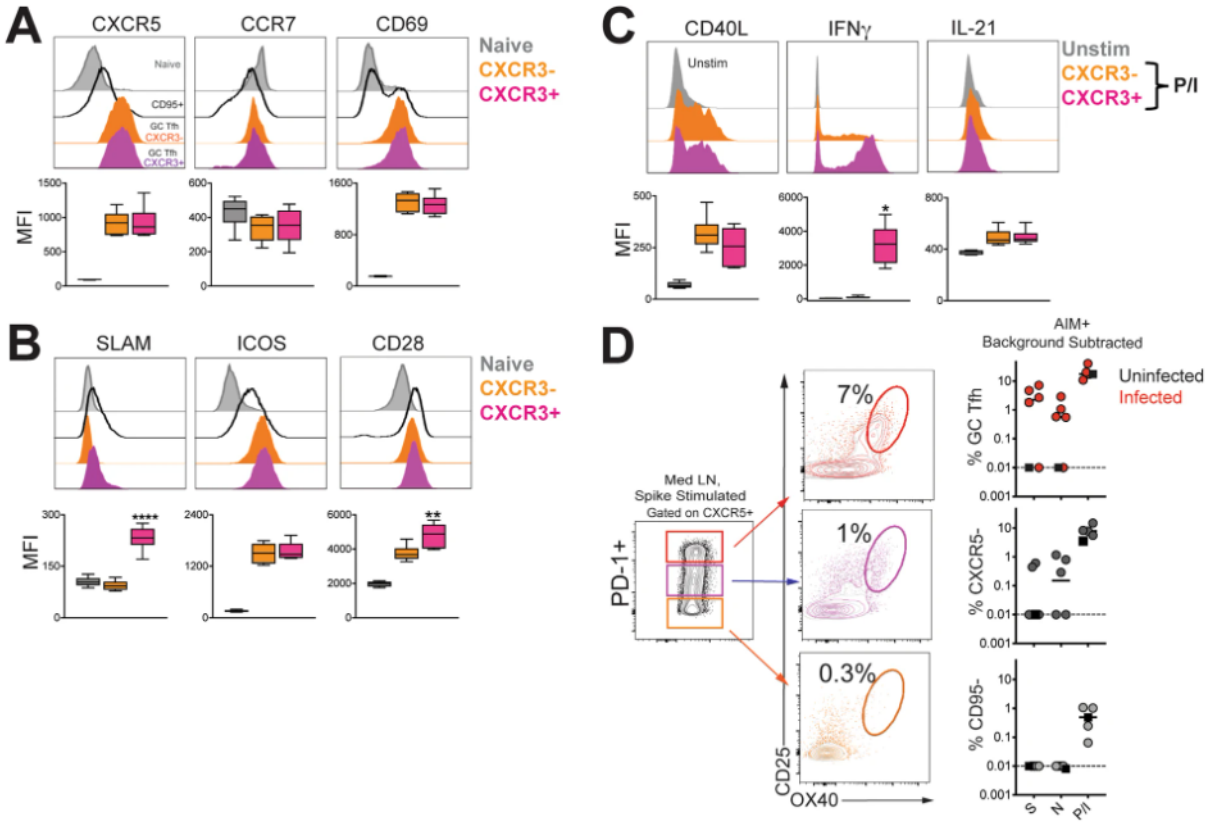

A Median fluorescence intensity (MFI) of CXCR5, CCR7, CD69 and **B** SLAM, ICOS, CD28 within CXCR3$^-$ (orange) and CXCR3$^+$ (magenta) GC T_{fh} cells in spleen following SARS-CoV-2 infection. Naive CD4 T cells in spleen shown for comparison (grey) (SLAM; $^{****}p < 0.0001$ CXCR3+ relative to naive and CXCR3– using a paired two-tailed *t* test, CD28; $^{**}p = 0.001$ CXCR3+ subset relative to naive and CXCR3- using a paired two-tailed *t* test) **C** Following PMA/Ionomycin stimulation, CD40L, IFNγ, and IL-21 expression shown across GC T_{fh} subsets. Unstimulated cells shown in gray (IFNG; $^{**}p = 0.0012$ CXCR3+ relative to CXCR3– using a paired two-tailed *t* test). Box-whiskers plot shows range of data, bounds of the box extend from the 25th to 75th percentile, line in box is plotted at the median. **D** Flow plot of PD-1$^+$ CXCR5$^+$ T_{fh} subsets shows AIM+ cells following stimulation with spike (S); scatter plot shows specificity of GC T_{fh} cells and CXCR5$^-$ cells to SARS-CoV-2 S and nucleocapsid (N), and responses to PMA/Ionomycin. CD95- naive CD4 T cell shown for comparison. The dashed line represents undetectable responses assigned a value of 0.01%. Black squares denote SARS-CoV-2 unexposed animals. Fluorochromes used were CD40L-APC; remaining as stated in previous panels.

Fig. 8: SARS-CoV-2 infection induces germinal center responses targeting spike (S) and nucleocapsid (N) in mediastinal lymph nodes.

CHARACTERIZATION OF HANDHELD DISINFECTANT SPRAYERS FOR EFFECTIVE SURFACE DECONTAMINATION TO MITIGATE SARS-COV-2 TRANSMISSION

Kim SC, Kwak DB, Kuehn T, Pui DYH.. Infect Control Hosp Epidemiol. 2021 Jan 13:1-7. doi: 10.1017/ice.2020.1423. Online ahead of print.
Level of Evidence: 5 - Modeling

BLUF

Mechanical engineers from the University of Minnesota and Chinese University of Hong Kong evaluated the performance of handheld disinfectant sprayers (trigger and electrostatic sprayers with and without electrostatic charging) by characterizing how each sprayer deposited disinfectant on desks (Figure 1). They observed the most uniform coverage when using an electrostatic sprayer from the front of a surface with a lateral swaying motion. Trigger sprayers did not spread disinfectant uniformly, thus authors recommend against their use in high-volume settings and suggest electrostatic sprayers be used with the above technique to optimally disinfect surfaces.

ABSTRACT

With schools reopening, an increasing number of custodians are applying disinfectant spray methods to decontaminate frequently touched surfaces, including school supplies, walls, desks, and chairs, to mitigate SARS-CoV-2 virus transmission between students, and teachers and students in the classroom. In this research, we present a novel characterization method to evaluate disinfectant droplet size and coverage for two types of commonly used disinfectant sprayers and suggest the optimum application practice for them.

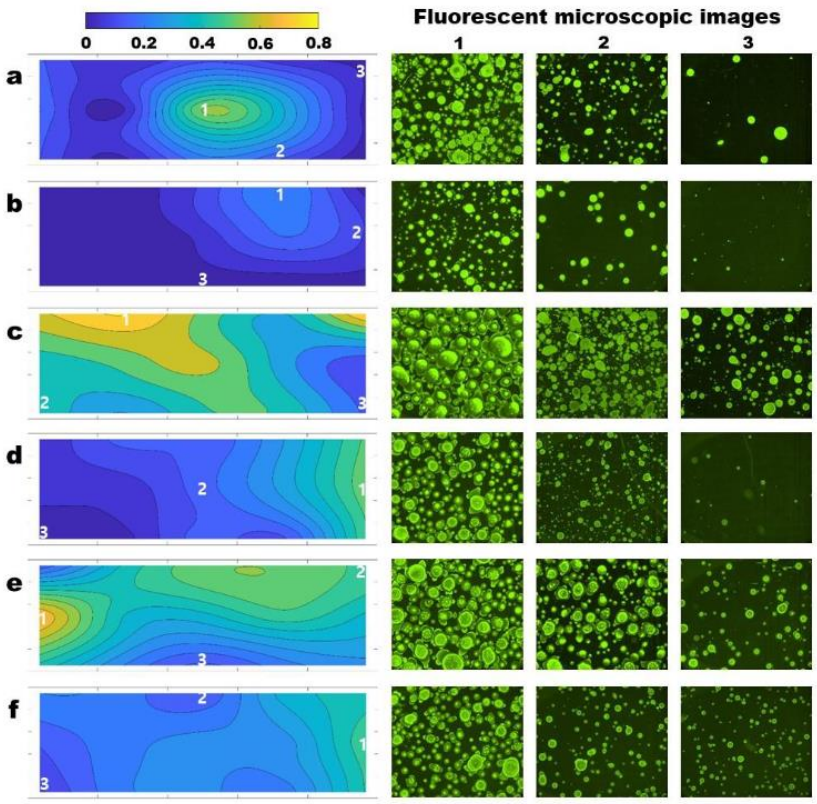

Figure 1.Deposition profiles and fluorescent microscopic images of disinfectant droplets collected on a classroom desk with various sprayer types and spray directions (Front: from top of the figure, Side: from right of the figure). The droplet depositions were sampled at 15 locations and the microscopic images that show the highest(1), medium (2) and lowest (3) depositions from each case are shown on the right. (a) Trigger sprayer (Front), (b) Trigger sprayer (Side), (c) Electrostatic sprayer with charge On (Front), (d) Electrostatic sprayer with charge On (Side), (e) Electrostatic sprayer with charge Off (Front), and (f) Electrostatic sprayer with charge Off (Side)The contour color bar represents local disinfectant coverage.

SHOULD CT BE USED FOR THE DIAGNOSIS OF RT-PCR NEGATIVE SUSPECTED COVID-19 PATIENTS?

Rona G, Arifoğlu M, Voyvoda N, Batırel A.. Clin Respir J. 2021 Jan 23. doi: 10.1111/crj.13332. Online ahead of print.
Level of Evidence: 3 - Non-consecutive studies, or studies without consistently applied reference standards

BLUF

Radiologists and infectious disease physicians from the University of Health Sciences in Turkey analyzed computed tomography (CT) imaging in 338 patients with suspected COVID-19 (Table 1) to evaluate the diagnostic utility of CT imaging in patients who tested negative for SARS-CoV-2 via reverse transcription-polymerase chain reaction. Because only 32.24% (n=109) of patients had typical CT findings (see summary)(Table 2), authors suggest the diagnostic value of CT in this patient population is low.

SUMMARY

Based on the Radiological Society of North America Expert Consensus Statement on Reporting Chest CT Findings Related to COVID-19, CT findings were classified into typical for COVID-19, indeterminate for COVID-19, atypical for COVID-19 and negative for pneumonia.

Additionally, patients with the following were considered to have typical findings:
- bilateral, peripheral ground-glass opacity (accompanied by consolidation or not)
- finding of of organized pneumonia (such as reversed halo sign)

ABSTRACT

INTRODUCTION: The diagnosis of patients with Coronavirus disease 2019 suspicion (COVID-19) but negative reverse transcriptase-polymerase chain reaction (RT-PCR) test is challenging. OBJECTIVE: We aimed to investigate the diagnostic value of chest computed tomography (CT) in RT-PCR negative patients with suspected COVID-19. MATERIALS AND METHODS: The study included patients who were admitted to our hospital with suspicion of COVID-19 between April 1 and April 30, 2020, who tested negative after RT-PCR test, and who underwent CT. Initial CT findings were classified as typical, indeterminate, atypical for COVID-19, and negative for pneumonia. Incidental findings on CT were noted. RESULTS: Of the 338 patients with a mean age of 57 years (min 18 years -max 96 years), 168 (%49.70) were male and 170 (%50.29) were female. The most common symptoms were cough (58.87%), fever (40.82%), and dyspnea (39.34%). The CT findings were typical for COVID-19 in 109 (32.24%) patients, indeterminate in 47 (13.90%) patients, and atypical in 77 (22.78%) patients. The CT findings of 105 (31.06%) patients were negative for pneumonia. Incidental lung nodules suspicious of malignancy were identified in 7 patients. Seventy-seven patients (%22.78) had extrapulmonary incidental findings. CONCLUSION: The diagnostic value of CT in RT-PCR negative patients with suspected COVID-19 is not very high. Based on clinical, laboratory, and chest x-ray findings, it may be more appropriate to refer patients to CT after the first triage, when necessary.

Characteristics	All Patients (n=338)
Age	
Mean	57
Range	18-96
Sex, n (%)	
Male	168 (49.70)
Female	170 (50.29)
Symptoms at presentation, n (%)	
Fever	138 (40.82)
Cough	199 (58.87)
Dyspnea	133 (39.34)
Sore throat	25 (7.39)
Loss of taste-smell	4 (1.18)
Headache	25 (7.39)
Gastrointestinal symptoms (nausea-vomiting, diarrhea)	46 (13.60)
Myalgia	79 (23.37)
Chest and back pain	23 (6.80)
No symptoms	5 (1.47)

Table 1: Demographic and clinical characteristics of patients

Table 2: Classification of patients by CT findings

	Typical for COVID-19, n (%)	Indeterminate for COVID-19, n (%)	Atypical for COVID-19, n (%)	Negative for penumonia, n (%)
All patients (n:338)	109 (32.24)	47 (13.90)	77 (22.78)	105 (31.06)
Patients with fever (n:138)	44 (31.88)	22 (15.94)	23 (16.66)	49 (35.50)
Patients with fever and cough(n:79)	26 (32.91)	13 (16.45)	13 (16.45)	27 (34.17)

PERFORMING POINT-OF-CARE MOLECULAR TESTING FOR SARS-COV-2 WITH RNA EXTRACTION AND ISOTHERMAL AMPLIFICATION

Garneret P, Coz E, Martin E, Manuguerra JC, Brient-Litzler E, Enouf V, González Obando DF, Olivo-Marin JC, Monti F, van der Werf S, Vanhomwegen J, Tabeling P.. PLoS One. 2021 Jan 11;16(1):e0243712. doi: 10.1371/journal.pone.0243712. eCollection 2021.
Level of Evidence: 4 - Case-control studies, or "poor or non-independent reference standard

BLUF

A team from the Industrial Physics and Chemistry Higher Educational Institution and Pasteur Institutes in Paris assessed the diagnostic performance of a novel device called COVIDISC (Fig. 3), which combines nucleic acid extraction, RT-LAMP and naked-eye visualization to detect SARS-CoV-2 (Fig. 1). Using SARS-CoV-2 positive swab eluates from a biobank, they found it capable of detecting a viral load of 1 copy per microliter of sample (Fig. 2) with a specificity of 100% in under an hour. Because its performance was comparable to RT-PCR, authors suggest COVIDISC offers a low-cost, easy to use testing platform to rapidly detect SARS-CoV-2.

ABSTRACT

To respond to the urgent need for COVID-19 testing, countries perform nucleic acid amplification tests (NAAT) for the detection of SARS-CoV-2 in centralized laboratories. Real-time RT-PCR (Reverse transcription-Polymerase Chain Reaction), used to amplify and detect the viral RNA., is considered, as the current gold standard for diagnostics. It is an efficient process, but the complex engineering required for automated RNA extraction and temperature cycling makes it incompatible for use in point of care settings [1]. In the present work, by harnessing progress made in the past two decades in isothermal amplification and paper microfluidics, we created a portable test, in which SARS-CoV-2 RNA is extracted, amplified isothermally by RT-LAMP (Loop-mediated Isothermal Amplification), and detected using intercalating dyes or fluorescent probes. Depending on the viral load in the tested samples, the detection takes between twenty minutes and one hour. Using a set of 16 pools of naso-pharyngal swab eluates, we estimated a limit of detection comparable to real-time RT-PCR (i.e. 1 genome copies per microliter of clinical sample) and no cross-reaction with eight major respiratory viruses currently circulating in Europe. We designed and fabricated an easy-to-use portable device called "COVIDISC" to carry out the test at the point of care. The low cost of the materials along with the absence of complex equipment will expedite the widespread dissemination of this device. What is proposed here is a new efficient tool to help managing the pandemics.

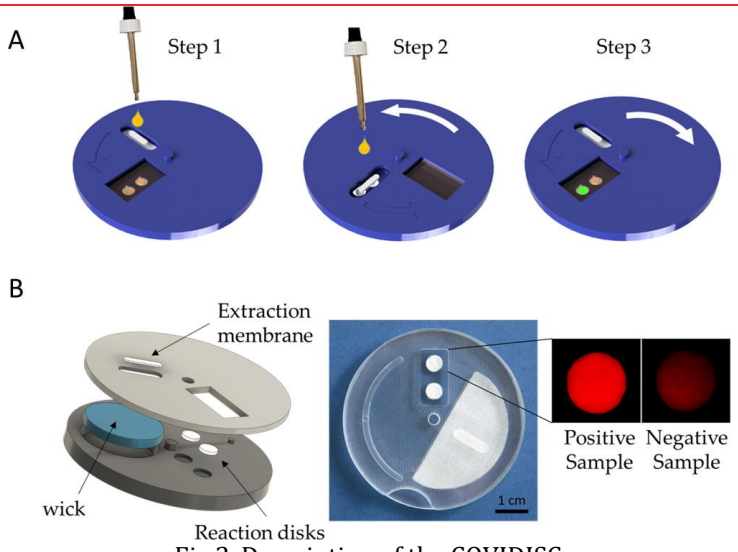

Fig 3. Description of the COVIDISC.

A–COVIDISC workflow decomposed in three steps (the three steps include the six steps of Fig 1, in the same the workflow): 1 –injection, washing (fluids flow through the capture membrane and get absorbed by capillarity in the absorbent wick (in blue)), drying. 2—Disk rotation and elution; 3 –Disk counter-rotation, coverage of the reaction zone by a PCR sealing film, heating, amplification and readout. B–Left: Exploded structure of the device. Center: Picture of a prototype. Right: QUASR readout photograph of a test on RNA extracts of SARS-CoV-2, processed as in Fig 3A; (left) Positive sample; (right) negative sample.

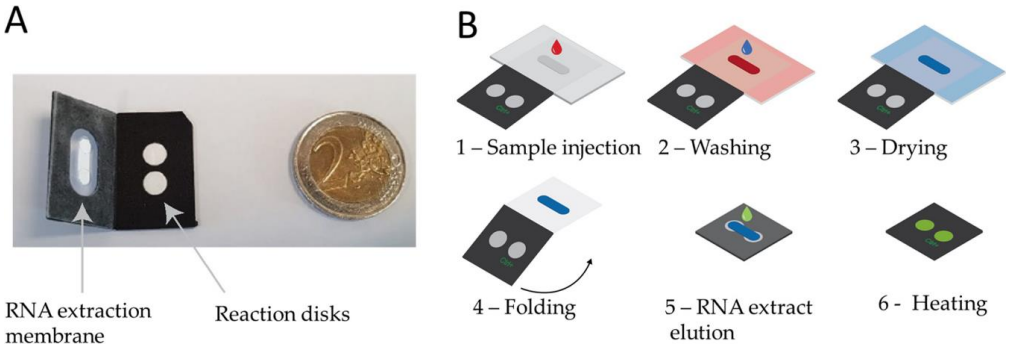

Fig 1. Laboratory device and workflow.

A: Two sheets of polypropylene (black) in which pretreated pieces of glass fiber (in white) are incorporated. B: Mode of operation. 1 –The sample, in which the virus has been lysed, is injected onto the extraction membrane. 2 –Washing. 3 –Drying of the extraction membrane. 4 –Folding of the device in such a way that the extraction membrane comes into contact with the two reaction disks. On both disk is freeze-dried the LAMP mix and primers (Covid-19 and human 18S RNA for the test and control disk respectively) permiting reverse transcription and amplification. 5 –Elution of the RNA from the capture membrane to the reaction disks, then, sealing with PCR tape 6 –Heating at 65°C. Read-out in real time with an intercalating agent (SYTO82).

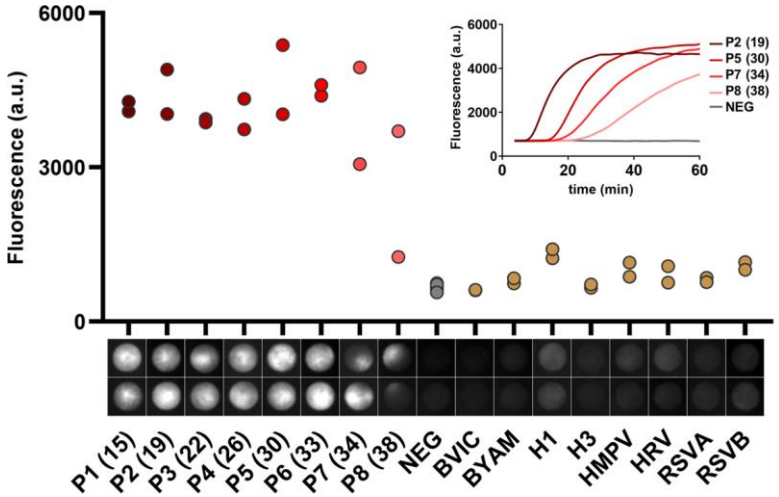

Fig 2. Detection of SARS-CoV2 in clinical samples, analytical performances of the test: Analytical sensitivity and Specificity end point (t = 60 min) measurements obtained for SARS-CoV-2 positive samples P1-P8 (SARS-CoV-2 RT-PCR Ct values in parenthesis), negative samples (individuals with a negative SARS-CoV-2 RT-PCR) and, on the right part, patients diagnosed with other respiratory infections.

The low intensity level measured on the negative samples (grey dots) corresponds to background fluorescence. The internal controls (RNA 18s) are displayed in S1 Fig in S1 File. At the bottom, series of disk images obtained at the end point, each vertical pair corresponding to duplicate assays. (Insert) RT-LAMP amplification curves obtained by real-time monitoring of the fluorescence produced by an intercalating dye (SYTO-82).

ACKNOWLEDGEMENTS

CONTRIBUTORS

Brad Mott
Julia Ghering
Michael Wang
Nicolas Longobardi

EDITORS

Maresa Woodfield

SENIOR EDITORS

Avery Forrow

SENIOR EXECUTIVE EDITOR

Sangeetha Thevuthasan

CHIEF EDITOR

Jackson Schmidt

ADVISOR

Will Smith